Mon. Not. R. Astron. Soc. **000**, 000–000 (0000)   Printed 22 September 1997

Evidence for pole switching in the magnetic cataclysmic variable BY Camelopardalis

Paul A. Mason[1,2], Gavin Ramsay[3,4], Ivan Andronov[5], Sergey Kolesnikov[5], Nickolay Shakhovskoy [6], Elana Pavlenko[6]

[1] *Case Western Reserve University, Dept. of Astronomy, Cleveland, OH 44106, USA*
[2] *New Mexico State University, Dept. of Astronomy, Box 30001, Dept. 4500, Las Cruces, NM, 88003 USA, pmason@nmsu.edu*
[3] *Astronomical Institute, University of Utrecht, Postbus 80000, 3508 TA Utrecht, The Netherlands*
[4] *Mullard Space Science Lab, University College London, Holmbury St. Mary, Dorking, Surrey, RH5 6NT, gtbr@mssl.ucl.ac.uk*
[5] *Odessa Astronomical Observatory, Odessa University, Shevchenko Park, 270014 Odessa, Ukraine*
[6] *Crimean Astrophysical Observatory, P/O Nauchny, 334413 Crimea, Ukraine*

Accepted: 1997 Sept 22

ABSTRACT

An analysis of X-ray and optical light curves of the magnetic cataclysmic variable (MCV) BY Cam is presented. This system is one of 3 MCVs in which the spin period of the white dwarf and the binary orbital period differ by $\sim$1%. As such these 'BY Cam' stars are important objects with which to probe the field structure of the magnetic white dwarf and ultimately the nature of synchronisation of AM Her binaries. We confirm asynchronous rotation of the magnetic white dwarf with respect to the binary. We find evidence that the accretion stream accretes directly onto the white dwarf as in AM Her systems, but further, the stream impacts onto different magnetic poles over the course of the beat period. We present evidence that the optical and hard X-ray light curves modulate in phase, but together they are out of phase with the soft X-ray light curve. We confirm the spin down of the white dwarf which is expected to lead to the synchronisation of the spin and orbital periods of BY Cam.

Key words: Stars: AM Her stars - stars: magnetic fields - stars: variables: other - X-rays: stars - stars: individual: BY Cam

1 INTRODUCTION

Magnetic Cataclysmic variables (MCVs) are binary systems containing a white dwarf primary which has a strong (1–230 MG) magnetic field and a Roche-lobe filling red dwarf secondary. Those systems in which the white dwarf rotates in phase-locked synchronism with the binary period are called AM Her binaries after their prototype, or polars, since they are highly polarised in the optical (see the reviews by Cropper 1990 and Beuermann & Burwitz 1995). The DQ Her binaries and/or Intermediate Polars (IPs) are those MCVs in which the rotation period of the white dwarf is not synchronised with the binary period (see Patterson 1994 for a review). In addition to these two groups there is another group which although has many properties similar to AM Hers have white dwarfs with rotation periods $\sim$1% different than the binary orbital period. These systems have been called the asynchronous Polars or 'BY Cam stars' (Patterson et al. 1995).

While many MCVs are described as 'enigmatic', BY Cam is one of the most deserving. Its circularly polarised light curve in particular is very variable on time scales of days to weeks (Mason, Liebert, and Schmidt, 1989). Spectroscopic observations have provided the best determination of the orbital period (P_{orb}=201.26 min: Sauter 1992, and Mason 1996), while photometric and polarimetric observations give the spin period of the white dwarf as P_{spin} = 199.3303 min, (Mason, Liebert, and Schmidt 1989, Mason et al. 1995). These results along with the X-ray period analysis of this paper confirm the suggestion of Silber et al. (1992) that white dwarf in BY Cam is rotating asynchronously (by $\sim$1%). Studies of the long term photo-polarimetric behaviour (Mason and Chanmugam 1992, Mason et al. 1995) suggest that the white dwarf rotation period is increasing at a rate of $\sim$0.1 sec/yr due to the synchronising magnetic torque.

In this paper we investigate the time-dependent nature of the X-ray and optical periods of BY Cam. We have analysed all available X-ray photometric time-series data. In addition, we have obtained new optical data and incorporated results from previous optical studies. We interpret these data in terms of the theoretical power spectra of Wynn and King (1992) who suggest that in an asynchronous stream accreting MCV, power at the spin frequency may not be seen in X-ray (and presumably optical) photometry. Hence, the spin period might not be readily observed without extensive polarisation measurements such as those presented in Mason, Liebert, and Schmidt, (1989) or if the photometry covers an interval which is short compared to the beat period (see §3.1).

2 OBSERVATIONS

2.1 X-ray Observations

In this study we examine data of BY Cam obtained using *EXOSAT*, *Ginga*, *ROSAT*, *BBXRT* and *ASCA*: Table 1 lists the dates of observations. Various aspects of these data have been reported elsewhere (e.g. *EXOSAT*: Shrader et al. 1988; *Ginga:* Ishida et al. 1991; *BBXRT*: Kallman et al. 1993; *ROSAT:* Ramsay et al. 1994; *ASCA:* Kallman et al. 1996). Pre-reduced (i.e. background subtracted etc.) data were extracted from the *EXOSAT* archive, while raw data were taken from the *ROSAT* and *Ginga* data archives and reduced in the usual manner. The reduced *BBXRT* and *ASCA* light curves were kindly supplied by Dr. Tim Kallman. In this paper we analyse these data again with the aim of investigating the time variations in detail.

We show, in figure 1, the X-ray light curves from Ginga, *ROSAT* and *ASCA*. The light curves are remarkably variable: in the first half of the observation made using *Ginga*, the spin period of the white dwarf was seen as a modulation in the light curve. However, in the second half the modulation disappeared and the source became significantly brighter. This bright unmodulated behaviour was called the flare state (Ishida et al. 1991). Again in the *ROSAT* data (figure 1: middle panel), there is a very bright flare state.

We can compare the mean brightness of BY Cam when it was observed in X-rays using the different satellites by assuming a spectrum typical to that found by Ramsay et al. (1994) (e.g. an absorbed blackbody plus thermal bremsstrahlung with kT_{bb} =50eV, kT_{tb}=30keV and $N_H = 2 \times 10^{20}$ cm^{-2}). We find that the mean brightness varies by a factor of $\sim$2. This is much lower than observed in other (synchronous) AM Her binaries, especially AM Her itself, which has been seen to vary by several orders of magnitude on time scales of months (e.g. Ramsay, Cropper & Mason 1995). The fact that BY Cam has a much lower mean range may simply be due to spectral changes in AM Her near the edge of the *ROSAT* bandpass. We go on to analyse these light curves in detail in §3.1.

2.2 Optical Observations

Optical monitoring of BY Cam has taken place each observing season from 1987 until 1995 with a general increase in the data collection rate. We have obtained a large amount of data thanks to the co-operation of many observers and incorporated previously published data of Mason, Liebert, and Schmidt (1989) and Silber et al. (1992). White-light and *UBVRI* photometry and polarimetry make up this database which now includes over 70,000 points. The largest and most informative subset is the *V*-band observations with over 25,000 data points. Most of the *V*-band data were obtained as a result of the 'Noah' collaboration (Silber et al. 1997). The rest of the previously unpublished data were obtained by some of us, IA, SK, NS, and EP during a multi-season *UBVRI* circular polarisation study using the Crimean Astrophysical Observatory (CrAO) 1.25 m and other smaller telescopes or by PM using the 61 inch telescope of the University of Arizona Observatories and the Burrell Schmidt telescope of Case Western Reserve University.

Satellite	Date of observation	Energy range
EXOSAT LE	7–9/10/1985	0.2–1.0keV
EXOSAT ME	7–9/10/1985	1–8keV
Ginga	7–10/2/1988	2–37keV
BBXRT	2–11/12/1990	0.3–12keV
ROSAT	9–14/3/1991	0.1-2.0keV
ASCA	10-11/3/1994	0.5–12keV

Table 1. The observations of BY Cam in X-rays. The dates when the observation took place along with the satellites energy range are shown.

3 PHOTOMETRIC TIME-SERIES DATA ANALYSIS

3.1 The X-ray time-series analysis

The fact that the X-ray data typically consist of short sections of data spread over several days make an analysis of the time series difficult when looking for variations on time scales of hours to days. The longest (2.92 days with 1314 data points) nearly continuous observing session in any bandpass is the *Ginga* observations made during 8–10 February 1988; this is also the highest energy (2-37 keV) data available. These data are nearly continuous except for periodic gaps due to Earth occultation during each orbit of the satellite. The time resolution of these data varies between 0.5 and 16 seconds (neglecting large gaps). Figure 2a shows the discrete Fourier transform periodogram of the *Ginga* data. The strong sharp power spike seen near 95 minutes reflects the orbital period of the satellite. This feature as well as one-day aliases flanking a strong signal near 200 minutes are removed using the CLEAN algorithm (Högbom 1974). Figures 2b & c show the CLEANed periodogram which displays only one significant power spike, located near 198 minutes. The asymmetric appearance may reflect either the presence of two closely space unresolved frequencies or the time evolution of a single frequency. A similar result is obtained using the phase dispersion minimisation method of Stellingwerf (1975).

In figure 3 the *Ginga* data is shown with a best-fit sine function. The best-fit period is 199.5 $\pm$ 0.8 min. The X-ray flux varies by a factor of about 4 over the periodic cycle and, except for briefly during the first part of the observation, a significant flux is seen throughout the observation. In addition the overall flux level increased during the last half of the observation and during that time the periodicity is weaker. Silber et al. (1992) used the Stellingwerf method on *Ginga* data covering the interval over which the signal

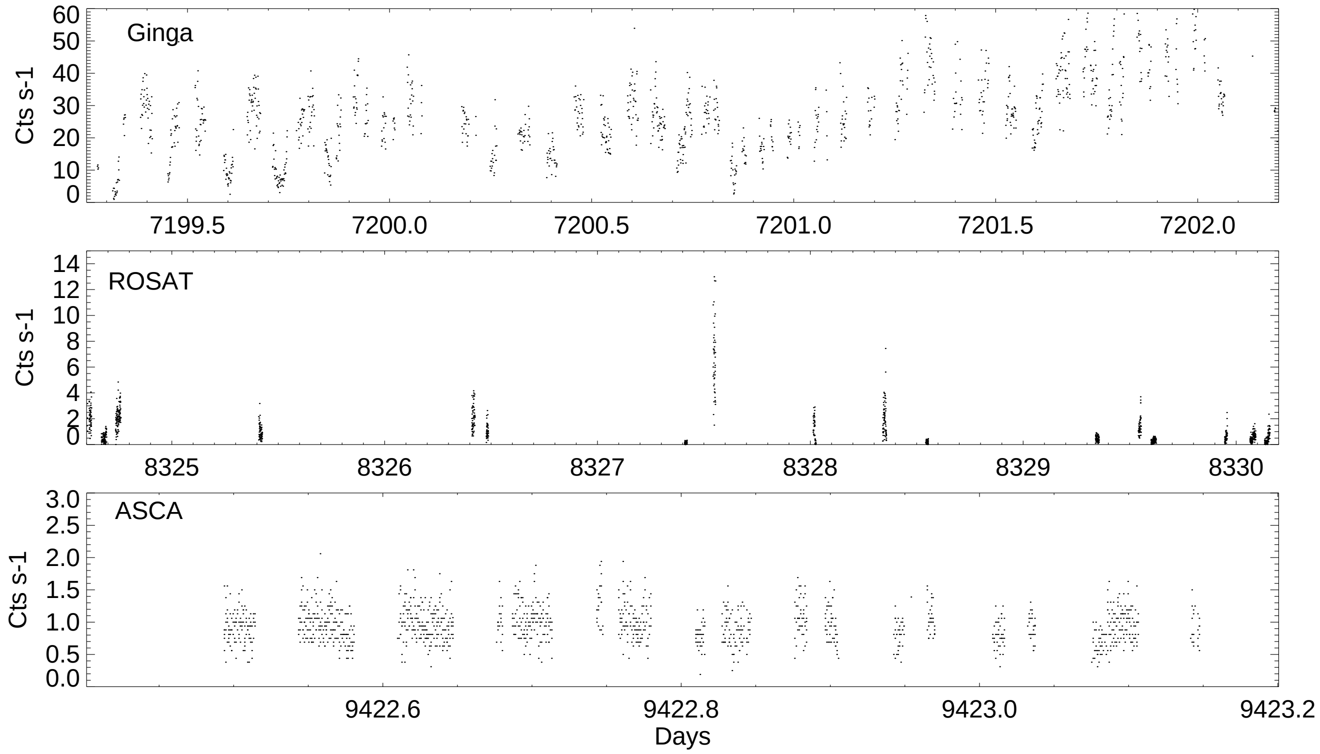

Figure 1. The X-ray light curves of BY Cam obtained using *Ginga*, *ROSAT* and *ASCA*. Observation times are given as HJD-2440000. Note the bright flare states in the *Ginga* and *ROSAT* light curves and that the three plots have very different temporal scales.

is periodic, namely 1988 February 7.7-9.5 (HJD 2447199.2-2447201.0) and obtained a period of 3.324 ± 0.008 hr which equals 199.44 ± 0.48 mins for this so called 'pulsed state'.

In order to investigate the time-dependence of this periodicity we calculated short-time Fourier periodograms by stepping through subsets of the data. The results are shown in figure 4. Each periodogram is calculated using 800 data points (1.8 days on average) and are not CLEANed. The individual periodograms are not independent as they are obtained using overlapping data. The transition from reasonably periodic (near the top of figure 4) to non-periodic behaviour is clearly seen. A probable explanation of this effect is the transition from a stable accretion geometry at the beginning of the observation to an unstable accretion geometry at the end, an effect predicted by non-instantaneous pole-switching.

In any stable accretion configuration one or more accretion regions will result in stable light curves showing the spin period, or in rare cases twice the spin period, of the white dwarf. If the system is observed during a transition in accretion state then the accretion geometry is unstable and the period might not appear in the data. Variations in the accretion rate (if fast enough) could produce a similar effect. However, this non-periodic behaviour more likely results from changes in the relative position of the accretion stream with respect to the white dwarf's magnetic field due to asynchronous rotation of the white dwarf with respect to the binary.

We searched for periodicities in the *EXOSAT* and *ROSAT* light curves using a Fourier transform. We found no evidence for periodicity anywhere near 200 minutes. This is probably due to the low sampling rate of *ROSAT* and the very low S/N inherent in the *EXOSAT* dataset. A strong signal in the *ROSAT* periodogram is seen at a period of about 395 minutes. This is about twice the period (197.4 min) detected as the strongest period in the optical photometry data from time-series longer than a few days as discussed in §3.2. The *ASCA* data covers approximately two orbital cycles and is not strongly periodic, while the *BBXRT* photometric time-series is too short to be useful.

3.2 The Optical time-series analysis

The Stellingwerf Θ-statistic (Stellingwerf 1975) was employed to search for periodicity in the entire set of optical photometry (covering roughly ten years) while keeping the different filter data separate. Fourier transform periodograms were calculated using various subsets of the data and were always found to be consistent with the Stellingwerf method. The Θ-statistic is calculated over a range of periods for the 'Noah' data obtained mainly at Manastash Ridge Observatory (MRO) using a V-band filter (see Silber

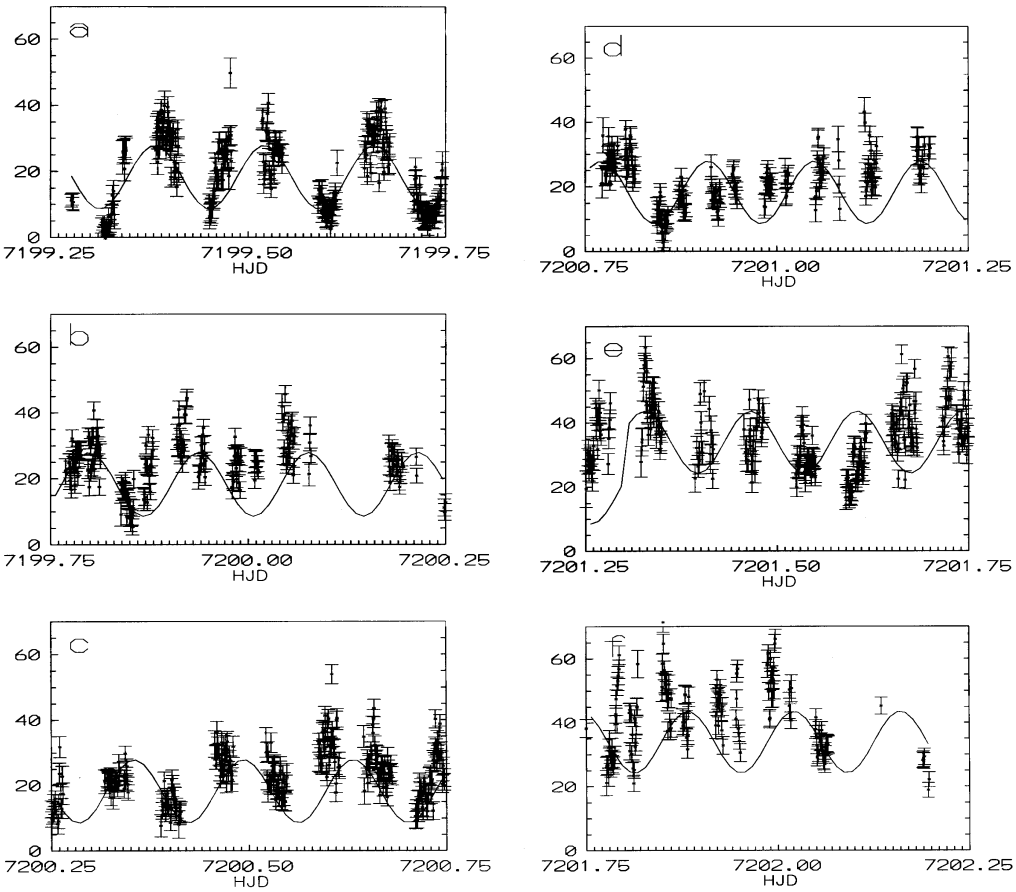

Figure 3. The *Ginga* data together with a best fit sine function. Notice that the fit is good near the beginning of the observation, but deteriorates until finally the data is no longer periodic. The mean value of the sign wave is allowed to suddenly shift to a higher level (see panel e) during the second half of the time-series for clarity; but the period, amplitude, and phase were free parameters in the solution. The best-fit period was 199.5 minutes.

et al. 1997 for details). Like Fourier transform periodograms of this and similar data sets there is a significant period at 0.1371 days (197.4 min). This period likely corresponds to the orbital side-band frequency ($f_{sb} = 2\omega - \Omega$) seen in power spectra models of Wynn and King (1992) designed to predict the power spectra of diskless asynchronously rotating MCVs.

Stellingwerf's phase dispersion minimisation technique was applied to each filter of the entire multi-year $UBVRI$ data. The largest of these data sets is the V-band data as it includes the Noah project data (Silber et al. 1997). There are no significant periods seen in either the U or B datasets. However, a period of 0.1371 days is evident in each of the $V, R,$ and I filter datasets. In figure 5, we show the $U, V,$ and I Stellingwerf periodograms. Since cyclotron emission is expected to dominate in the $V, R,$ and I bands this period is probably associated with the cyclotron emission region(s) located near the surface of the white dwarf. The lack of a coherent modulation at this period in U and B suggests that an additional source of radiation is significant in this part of the spectrum. In addition the cyclotron component is presumably much weaker at U and B as is expected for a MCV with the high magnetic field of BY Cam (Cropper et al. 1988). The result is that the U and to a lesser extent the B filter data lack significant periodic behaviour.

On five nights, in December 1994, long trains of equally spaced data were obtained using the Burrell Schmidt Telescope of Case Western Reserve University, by PM, using an R filter. The most stable of these light curves was obtained on 17 December 1994, yielding a period of 199.3 ± 1.5 min from several period determination methods. This result is in good agreement with the polarimetric period of Mason, Liebert, and Schmidt (1989). However, this period is significantly different from that found from data sets incorporating many nights of data such as that shown in figure 5. The Burrell Schmidt observations were the longest nights of data obtained by the Noah project (Silber et al. 1997). Unfortunately, night to night light curve instabilities prevent a more precise photometric spin period determination.

Period search methods were applied to the full 45 night Noah project data and the CLEANed periodogram is shown in figure 6. The significance level of the various peaks can be roughly judged by the noise level of the periodogram. The main power spike is at 197.4 ± 0.1 mins. The width of the this feature is considerably broadened by the phase shifts discussed in Silber et al. (1997) and reviewed later in this section. This period is inconsistent with the period found from the X-ray analysis above. In addition this period is significantly different from the short (single night) runs such as that obtained from the longest and most stable light curves obtained at the Burrell Schmidt Telescope and the polarisation obtained at the Steward Observatory

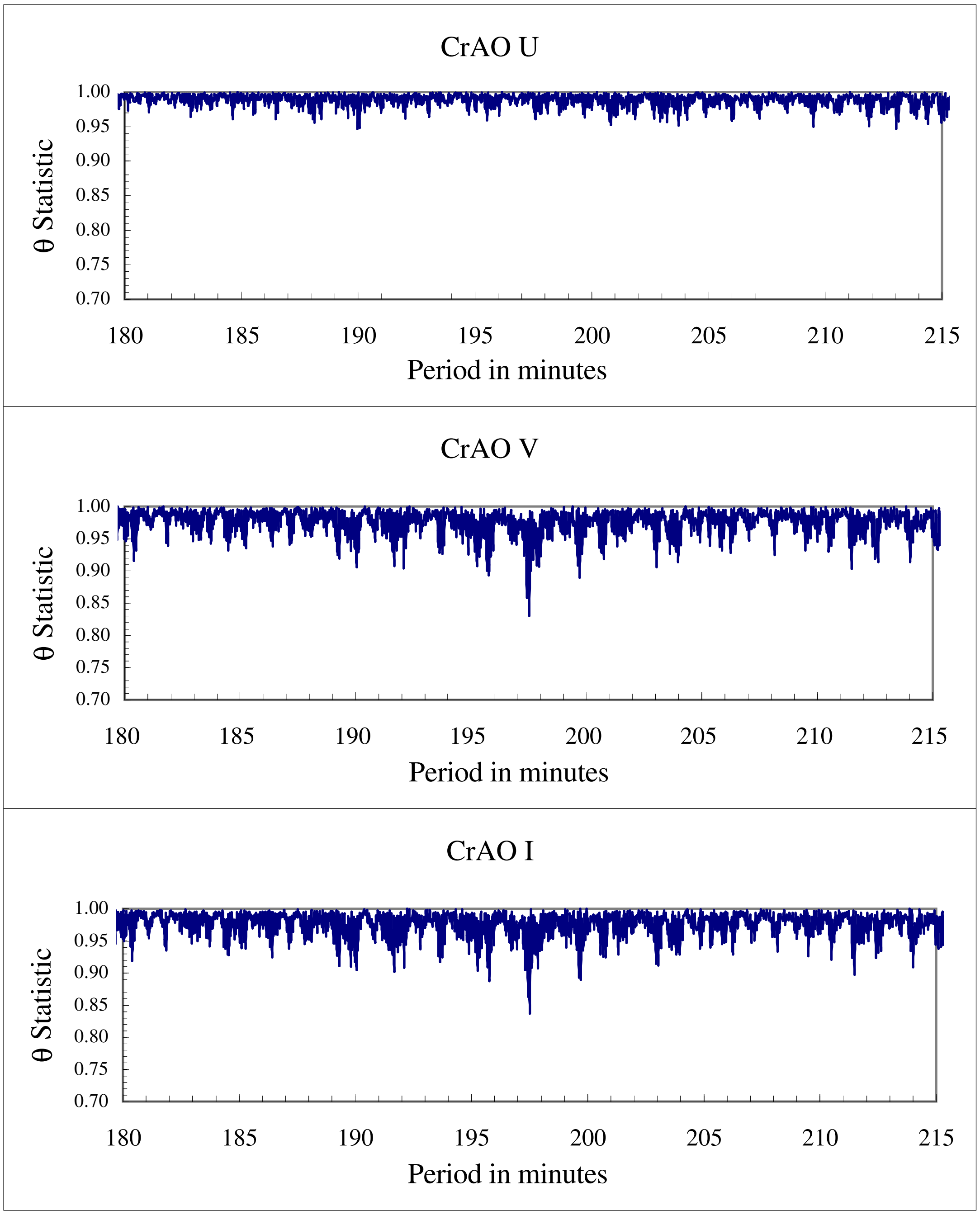

Figure 5. The Stellingwerf phase dispersion minimisation test for U, V and I data. No significant period appears in the U data. There is a significant period at 0.1371 days (197.4 min) in the V and I filter data. This is the same period seen in the 'Noah' project data.

2.3 meter telescope (Mason, Liebert, and Schmidt 1989). Power spikes at other frequencies are also shown, including the orbital period, the likely spin period, and an additional side-band period. The weight of evidence suggests that the photometric period determined from many nights of data is not due to the spin frequency of the white dwarf, but rather the $2\omega - \Omega$ orbital side-band frequency.

Silber et al. (1997) fitted the individual nightly light curves of the Noah data to sine-waves. They then compared the maxima of the individual sine wave fits to the overall best-fit in the form of an O − C diagram. They found that the individual light curves are periodically phase shifted with respect to the overall best-fit. The residuals were period searched by Silber et al. (1997) using the Stellingwerf method and a period of 7 days was seen in both the phase and amplitudes of the O − C residuals. This supports the suggestion of Mason et al. (1995) that the accretion geometry of BY Cam changes in a periodic manner.

The secular behaviour of the 197.4 minute periodicity is studied using the non-linear least squares method (Mason 1996). All of the V observations were combined with the white light photometry and fit with a sine function with a period which is allowed to vary linearly with time. A grid search in χ^2 space was performed using the period and the

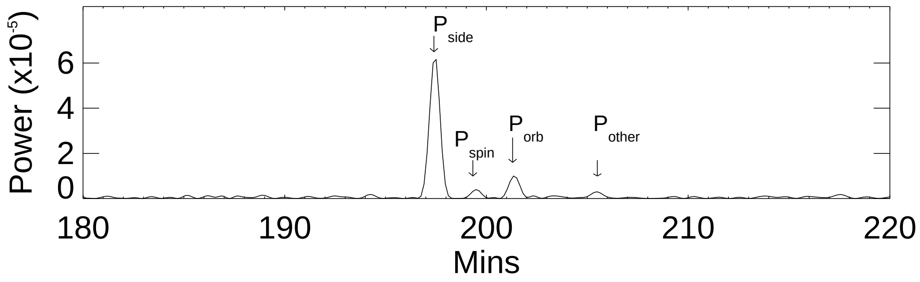

Figure 6. The CLEANed Fourier transform for the Noah set of optical data. The main spike is at 197.44 minutes. The 'other' period may be the $3\,\Omega - 2\omega$ frequency.

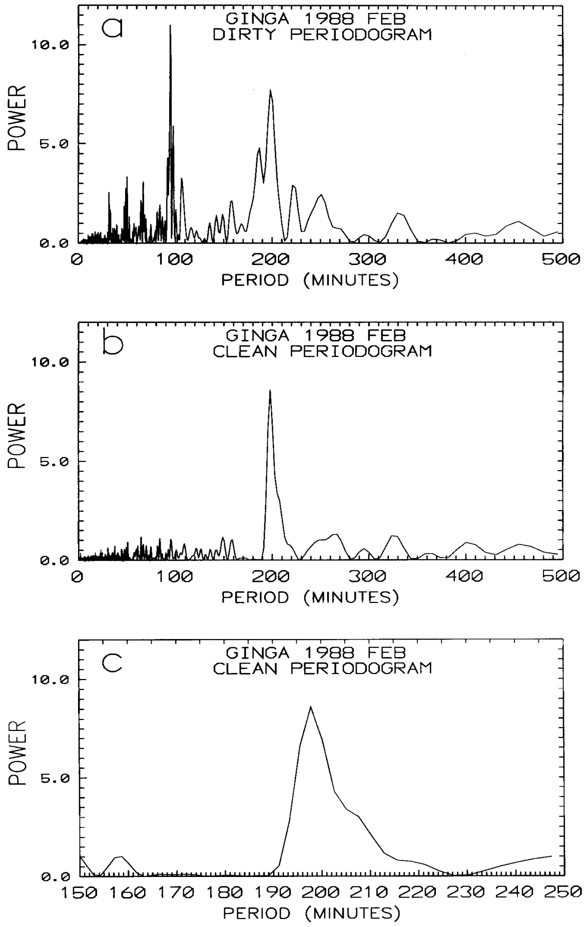

Figure 2. a): The Fourier transform periodogram of the *Ginga* data, b): the CLEANed transform, and c) as before but narrowing the period range. Only one significant period (198 min) is seen: it is likely the spin period of the white dwarf.

period derivative as input parameters and calculating a one-parameter fit where the only parameter to fit was the phase at JD 2449500 (chosen to be near the densest part of the data). The resulting contours in χ^2 space are examined to locate the lowest 'valley(s)'. Then a final non-linear least squares fit with all parameters set free and starting values near the lowest valley is performed. The best fit period and period derivative is P=197.438 ± 0.002 minutes (0.1371095 days) and dP/dt=0.26 ± 0.01 seconds/year, both at epoch HJD=2449500. We note that with the orbital period (Sauter 1992) and the relationship $f_{sb} = 2\omega - \Omega$ we arrive at a consistency with with the best choice ephemeris based on polarisation (Mason, Liebert, and Schmidt 1989) and (after dividing by 2) we obtain a new spin period derivative of 0.132 ± 0.005 seconds/year. The fact that the photometric period derivative must be twice the spin period derivative comes from assuming that the orbital period does not change significantly and differentiating $f_{sb} = 2\omega - \Omega$ with respect to time. The fact that the secular increase in the spin period produced phase displacements which were significantly greater than the amplitude of periodic shifts due to pole-switching, made this method of determining the spin period derivative possible. Because of these shifts, period and period derivative error estimates based on the chi-squared solution are unrealistic. Accordingly, we estimate our uncertainties by phasing the data with a range of periods and period derivatives to conservatively determine their range. The phase shifts at different epochs were clearly inconsistent with a constant period.

3.3 The folded X-ray and optical data

To look at the long term behaviour of the X-ray light curves and their relationship with the optical light curve we folded these data at the side-band period. All of the X-ray and optical data were taken over a period of >1day (apart from the *ASCA* data which covered only 0.7 day). We folded the data on the side band frequency $f_{sb} = 2\omega - \Omega$=197.438 mins where the folding epoch was near the midpoint of the data sets (JD=2447890.0).

Figure 7 shows the side-band folded optical data covering 45 days, and X-ray data obtained using *ASCA*, *ROSAT* and the *EXOSAT* LE and ME detectors. The Ginga data presented here and in Silber et al. 1992 was obtained simultaneously with optical data, so the phasing is unambiguous. Taking into account the possible phase error between the various datasets (<0.13 cycles), this figure may suggest that the optical and the hard X-ray (*Ginga* and the *EXOSAT* ME) folded light curves are in phase while the soft X-ray folded light curves are in phase (but with the secondary peak varying in strength) but out of phase with respect to the hard X-ray and optical light curves.

Our current understanding of the accretion mechanism in AM Her systems, is that the accretion stream is very inhomogeneous (e.g. Ramsay, Cropper & Mason 1995). A

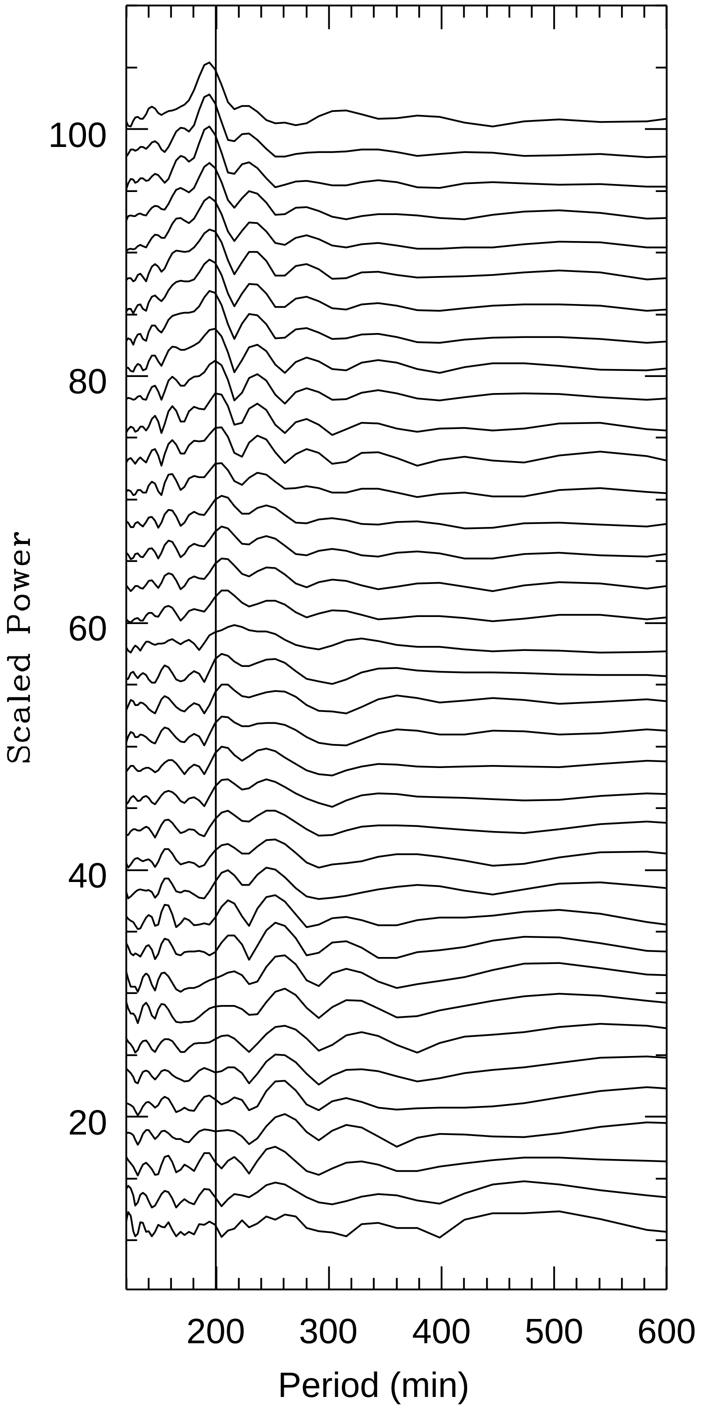

Figure 4. The Fourier transform of the *Ginga* data as a function of time. Time progresses from top to bottom. The transition from strictly periodic (near 200 minutes and the top of the figure) to non-periodic behaviour is clearly seen.

diffuse 'rain' of material in the stream shocks above the surface of the white dwarf generating hard X-rays and cyclotron radiation in the optical/IR. Blobs of material (which are thought to be present in the stream) with sufficiently high density will penetrate deep into the photosphere before being shocked, where their accretion energy is thermalised and emerges in soft X-rays or in the EUV. In this view the hard

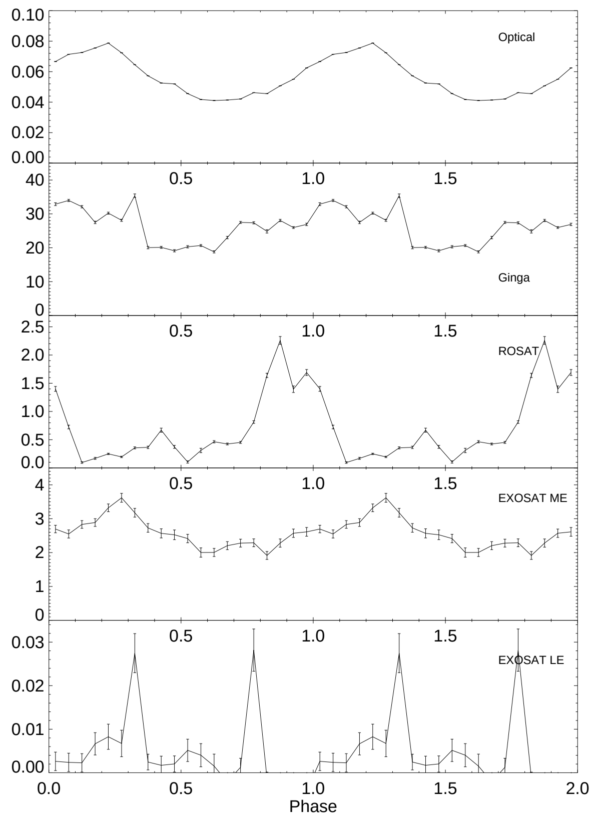

Figure 7. The optical and X-ray data folded on the side band period of 197.438 mins.

X-ray and optical flux is expected to be correlated to some degree, since they both originate from the 'rain' of accreting material. Although the above accretion scenario may be modified in the case of the asynchronous AM Her stars, it is expected to be applicable here.

The peak in the optical and hard X-ray light curves at ϕ ~0.2–0.3 suggests that the optical and hard X-ray flux originate from the same accretion pole (as expected from the view described above). However, the peak in soft X-rays at ϕ ~=0.85 indicates that soft X-rays are being emitted from a different pole than the pole producing the optical and hard X-rays. Further, the fact that a soft X-ray peak is seen at ϕ ~0.3 in the *EXOSAT* LE observation suggests that soft X-ray emission is also seen (at times) from both poles.

A separation of soft and hard X-ray emission has been seen in several other synchronous AM Her systems (eg QQ Vul: Beardmore et al 1995) which suggests the presence of two pole accretion and moreover implies different magnetic field strengths at each pole (to account for one pole being stronger in soft X-rays than hard X-rays). The latter observation indicates a more complex magnetic field than a simple pure dipole magnetic field. This is consistent with the suggestion of Wu and Mason (1996) that the magnetic field of BY Cam is better modelled with a dipole plus quadrupole magnetic field and the fact that the polarisation observations of Piirola et al. (1993) suggest the presence of a complex magnetic field.

4 DISCUSSION

We discuss our results within the framework of theoretical power spectra of stream accreting (i.e. diskless) asynchronous magnetic CVs of Wynn and King (1992). The power spectrum would reveal the spin frequency if the time interval over which the power spectrum is calculated is short compared to the beat period. Power spectra calculated over longer time intervals will include the effect of pole-switching. In addition, they find that the X-ray power spectra are strongly dependent on the binary inclination, i, and magnetic co-latitude, m.

In the case that $i+m+\beta<90^{\circ}$ where β is the opening angle defining the size of the polecap (and the two poles are diametrically opposed) one of the accretion regions will always be visible and the other will be behind the limb at all times (the 'one-visible-pole' model). In this case the light curve would be a square wave modulating at the spin-orbit beat $(\omega-\Omega)$ frequency. This is clearly not what is observed for BY Cam.

If on the other hand $i+m+\beta>90^{\circ}$, then both accretion poles would alternately be visible (but at opposite spin and beat phases). This is the 'two-visible-pole' model (again with diametrically opposed identical poles). Power spectra calculated over time intervals comparable to the beat period will include the effect of pole-switching and contain two major power peaks at the orbital frequency Ω and a spin-orbit side-band frequency $2\omega-\Omega$ with similar strengths (see figure 4 of Wynn and King) and virtually no power at the spin frequency. For a more complex model (i.e. non-diametrically opposed or non-identical poles) the symmetry is broken and the spin period becomes a significant feature in the power spectrum.

To interpret the BY Cam observations in terms of the Wynn and King 'two-visible-pole' model we first note that the X-ray and optical power spectra obtained from short (1–2 day) time-series display periods near 199.3 minutes while longer time-series yield a 197.4 minute period. This result suggests that the spin period of BY Cam is 199.33 minutes (Mason, Liebert and Schmidt 1989; §3.1) and the 197.4 minute period (Mason et al. 1995, Silber et al. 1997; §3.2) corresponds to the $2\omega-\Omega$ spin-orbit beat-frequency. The only problem with this interpretation is that equal power is expected at Ω and $2\omega-\Omega$ which is not observed. The only apparent way to reconcile this model with the observations is to require that the two poles (already assumed to have identical emission properties) also produce identical light curves. This is possible if both poles are located very near the spin equator of the white dwarf. For this special case the simple polecap model produces power at the $2\omega-\Omega$ frequency and not the orbital Ω frequency.

The alternative 'one-pole' model cannot explain the appearance of power near 199.32 minutes (the polarisation period of Mason, Liebert, and Schmidt 1989) in power spectra derived from short duration time-series such as the pulsed state Ginga data (Silber et al. 1992, see §3.1 and figure 3). However, uncertainties in these period determinations are large because they are based on such short (1–2 day) time-series and the power in the orbital and side-band are not equal as predicted in the Wynn and King models. Therefore, we cannot absolutely exclude the possibility that the 197.4 minute period is the spin period of the white dwarf and that pole switching takes place between poles separated by much less than 180° (see Silber et al. 1992 for details on the pole locations for this model; however, we consider this possibility unlikely because it cannot explain the 199.3 min period).

A multi-polar magnetic field model (Wu & Mason 1996, Wu & Wickramasinghe 1993) might naturally explain both of these later points. The reconciliation of this matter is vital, because the preferred model requires a strong quadrupole field component and is not consistent with a dipole or even an offset dipole magnetic field configuration (Wu and Mason 1996). If confirmed, this will be the first case of a polar possessing a multi-polar magnetic field since all other suggested multi-polar magnetic field polars cannot exclude the possibility of offset dipoles.

5 CONCLUSIONS

In conclusion, we have firm evidence that BY Cam is an asynchronous stream accreting magnetic CV. We suggest that pole-switching takes place because the light curve undergoes episodes of aperiodicity during which the light curve gradually changes shape while the accretion rate remains steady. We propose two models based on the theoretical power spectra of Wynn and King (1992). One of these models, where the spin period of the white dwarf is equal to the dominant spike in the (long term: > few days) power spectra, i.e. 197.4 minutes, we consider to be unlikely because it cannot explain the power at 199.3 minutes seen in the (short term: 1–2 day) power spectra. The other model in which the dominant spike in the power spectrum is a spin-orbit side-band frequency predicts that the spin period of the white dwarf is 199.3303 minutes (Mason, Liebert, and Schmidt 1989; Mason et al. 1995). This latter model requires that the two (main) accretion regions are approximately diametrically opposed and both are probably located near the spin equator of the white dwarf.

6 ACKNOWLEDGEMENTS

We would like to thank all the observers who contributed to the 'Noah' optical data set (see Silber et al. 1997 for the list of contributors) and Dr. Tim Kallman for kindly supplying us with the *ASCA* light curve of BY Cam. We thank the Crimean Astrophysical Observatory, Case Western Reserve University, and the University of Arizona for large allocations of observing time. PM thanks his Ph.D. thesis advisor Dr. George W. Collins, II for numerous fruitful discussions. We thank Dr. Mark Cropper and an anonymous referee for careful review and suggestions for the manuscript. This work was done while PM was a Towson memorial scholar at CWRU. GR would like to thank the European Union for a fellowship. This paper is based partially on data extracted from the UK *ROSAT* and *Ginga* data archive centre in Leicester.

7 REFERENCES

REFERENCES

Beardmore, A. P., Ramsay, G., Osborne, J. P., Mason, K. O., Nousek, J. A., Baluta, C., 1995, MNRAS, 273. 742

Beuermann, K., Burwitz, V., 1995, in Cape Workshop on MCVs, ASP Conf Ser, 85, 99

Cropper, M., Sp. Sci. Rev., 1991, 54, 195

Cropper et al. 1988, MNRAS, 236, 29P

Högbom, J. A., 1974, A&A Supp. 15, 417

Ishida, M., Silber, A., Bradt, H. V., Remillard, R. A., Makishima, K., and Ohashi, T., 1991, ApJ, 367, 270

Kallman, T. R. et al, 1993, ApJ, 411, 869

Kallman, T. R., Mukai, K., Schlegel, E. M., Paerels, F. B., 1996, ApJ, 466, 973

Mason, P. A., 1996, PhD thesis, Case Western Reserve University

Mason, P. A., Liebert J., Schmidt, G. D, 1989, ApJ, 346, 941

Mason, P. A., Chanmugam, G., 1992, in Vina del Mar workshop on CVs, ASP Conf Ser, 29, 216

Mason, P. A. et al 1995, in Cape Workshop on MCVs, ASP Conf Ser, 85, 496

Patterson, J., Skillman, D. R., Thorstensen, J., Hellier, C., 1995, PASP, 107, 307

Patterson, J., 1994, PASP, 106, 209

Piirola, V, Coyne, G., Takalo, L., Larsson, S., Vilhu, O., 1994, A&A, 283, 163

Sauter, L., 1992, BS thesis, MIT

Shrader, C. R., Remillard, R. A., Silber, A., McClintock, J. E. & Lamb, D. Q., 1988, in *A decade of UV astronomy with the IUE*, (ESA SP-281), Vol. 1, 137, ESA, Noordwijk

Silber, A., Bradt, H. V., Ishida, M., Ohashi, T., Remillard, R. A., 1992, ApJ, 389, 704

Silber, A. et al, 1997, MNRAS, 290, 25

Stellingwerf, R. F., 1975, ApJ, 199, 705

Ramsay, G., Mason, K. O., Cropper, M., Watson, M. G., Clayton, K. L., 1994, MNRAS, 270, 692

Ramsay, G., Cropper, M., Mason, K. O., 1995, MNRAS, 276, 1382

Wu, K., Mason, P. A., 1996, In Proc Keele Conf on CVs

Wu, K., Wickramasinghe, D. T., 1993, MNRAS, 260, 141

Wynn, G. A., King, A. R., 1992, MNRAS, 255, 83